

OPTIMIZATION AND GREEN SYNTHESIS OF SILVER AND GOLD NANO-PARTICLES DERIVED FROM *COLOCASIA ESCULENTA* ROOT EXTRACT AND THEIR POTENTIAL PHARMACOLOGICAL APPLICATIONS

Reshma Tendulkar^{a*}

(Received 01 November 2020) (Accepted 08 March 2023)

ABSTRACT

The broad array of potential applications of silver and gold nano-particles in diverse fields is well-known. The utilization of lethal reagents is included in the contemporary procedures of synthesizing nano-particles. In present times, there is necessity to augment novel mechanisms that lead to the synthesis of gold and silver nano-particles with the help of environmentally safe reagents. The reliable green synthesis of silver and gold nano-particles with the help of *Colocasia esculenta* root extract popularly called as Arvi, has been investigated here. The experimental procedure employed here to scrutinize and observe the synthesis of silver and gold nano-particles based on quantity is UV-Vis absorption spectroscopy. Surface Plasmon Resonance (SPR) was exhibited by UV/Vis spectrum for silver and gold nano-particles at 420 and 540 nanometers, respectively. The mean diameter of gold and silver nano-particles synthesized in the solution was found to be 85 nm and 105 nm, respectively. The particles that were synthesized had a spherical shape.

Keywords: Silver nano-particles, gold nano-particles, antimicrobial, antioxidant, *Colocasia esculenta*

INTRODUCTION

The branch of nanotechnology primarily explores the formation, categorization and use of the products in the scale of 0–99 nanometers. Nano-particles are employed to elucidate structures that naturally occur in nanometer size range¹. The metallic nano-particles portray high area to volume ratio and exhibit significant attributes in contrast with their counterparts². The synthesis of metallic nano-particles exhibits natural behavior; which is the salient attributes of nano-technology³. Contemporary procedures like physical and chemical formation of metallic nano-particles possess numerous drawbacks which includes the utilization of lethal chemicals such as reducing/ capping substances, high energy expenditure and hurdles in refinement⁴. Hepatotoxicity and renal toxicity are other major obstacles which are reported for metallic nano-particles which are synthesized using toxic chemicals; when administered through oral inhalation or subcutaneous route⁵. Due to numerous disadvantages of the contemporary chemical techniques; it is indeed inevitable to redesign and reinvent environmentally safe, cheap and biocompatible processes for synthesizing

metallic nano-particles with a narrowly utilitarian view⁶. The technique of green synthesis is most feasible and the best alternative procedure as compared to other chemical techniques⁷. Plants have the specialized potential to produce metallic nano-particles. This is recognized to be reduction of metals that is plant-mediated and relies on environment consisting of chemical components; this allows conversion of ions of metals to metallic nano-particles⁸. In addition to being utilized as a reductant, the plant extract is used as an agent for stabilization for metallic nano-particles.

This research article highlights *Colocasia esculenta* root facilitated synthesizing of metallic nano-particles and its conceivable significance in nano-medicine.

A tropical plant known as *C. esculenta* cultivated chiefly for its comestible corms, it is a root vegetable ordinarily acknowledged as Arvi, taro, or kalo in the Hawaiian language. It contains numerous species in the plant Araceae family; being primarily consumed for their corms, leaves and petioles.

MATERIALS AND METHODS

The roots of Arvi were acquired from a local seller of vegetable market in Mira Road, Mumbai. They underwent

^a Department of Pharmaceutical Chemistry, Vivekanand Education Society's College of Pharmacy, Chembur, Mumbai-400 074, India

*For Correspondence: E-mail: reshma.tendulkar@ves.ac.in

validation for their reliability with the species (*C. esculenta* included in the family Araceae). Ascorbic acid, silver nitrate and DPPH were obtained from Vaishali Chemicals in Maharashtra. The nutrient medium was obtained from HI MEDIA in Maharashtra.

Preparation of silver and gold nano-particles from root extract of *C. esculenta*

C. esculenta roots possess the ability to reduce ions of metals to metallic nano-particles. The formation of metallic silver and gold nano-particles has been claimed for their synthesis of the root extract of *C. esculenta*⁹.

The roots of *C. esculenta* were comprehensively cleansed with the help of distilled water in order to eliminate surface contaminations. The roots of Arvi were squashed and water of calculated volume was mixed. It was then heated on a magnetic stirrer at 75 °C for 25 minutes. After filtration, mixture was put through a technique of centrifugation; carried out at 10500 revolutions per minute (rpm) for 20 minutes in order for the sedimentation to occur. In order to completely eradicate impurities, the procured supernatant was strained by using Whatman no. 1 filter paper. It was then stored in refrigerator at a temperature of 4°C. It is used as a stabilizing and reducing agent.

Preparation of silver nitrate solution (1mM)¹⁰

Precisely weighed silver nitrate of 0.017 g was dissolved in 100 mL of distilled water to produce silver nitrate of the concentration 0.1 mM.

Preparation of chloroauric acid (CA) solution (1mM)¹¹

25 % Chloroauric acid (CA) weighing 0.034 g was diluted in 150 mL of distilled water to make chloroauric acid of concentration 1.2mM.

Synthesis of metallic gold and silver nano-particles from root extract of *C. esculenta*¹²

At room temperature, 50 mL solution of 1mM of metal salt solution and 30 mL root extract of *C. esculenta* were mixed. Under static conditions at room temperature, to circumvent the photo-activation of metal salts, the reaction mixture was incubated in the dark for 22 to 45 h. The end point for the synthesis of silver nano-particles was exhibited through color transformation from bright white to brownish yellow and for gold nano-particles from bright white to violet. It was known due to reduction of metal ions from +1 to 0 oxidation state; representing nano-particle synthesis. Nano-particles were segregated through

process of centrifugation technique at 12500 rpm for 35 minutes. The dispersion of metallic nano-particles was carried out in distilled water. They were later subjected to critical characterization and analysis. The procedure later included, incubation of the reaction mixtures with critical amount of concentrate at 24, 48, 72 and 96 h with a view of examining the outcome of reaction time. The reaction mixtures were incubated at temperatures such as 30, 50, 70 and 90 °C, the impact of higher temperature on the formation of metallic nano-particles was evaluated. The hydrogen ion concentration of the reaction was varied along with 0.2 N sodium hydroxide and 0.1 N hydrogen chloride, influence changing pH on the metallic nano-particles synthesis was examined. The impact of fluctuating the strength of CA and silver nitrate (AgNO₃) (3.24, 1.82 mM) formation of nano-particles researched independently of each other. The influence of extract volume added (2, 3, 4, 5 mL) to mixtures during formation of metallic nano-particle was investigated.

Categorization of silver nano-particles

The spectrum of nano-particles documented the range from 250 to 750 nm by utilizing SHIMADZU, UV-1800.

Observations of Field Emission Scanning Electron Microscopy (FESEM) and Transmission Electron Microscopy (TEM)

Field Emission Scanning Electron Microscopy (FESEM) was responsible for determining the structure and dimensions of metallic nano-particles. A droplet of aqueous dispersion of metallic nano-particles was filled at room temperature upon a copper grid was then made to dry for FESEM. Once the sample was dried completely, the micrographs were monitored utilizing FESEM (JEOL JSM-7600). Similarly, the analysis of Transmission Electron Microscopy (TEM) illustrations was accomplished. For a particular section, TEM (JEOL JSM) illustrations were monitored and the electron diffraction pattern obtained.

Analysis of the size of particles

The Z-average size and polydispersity Index (PDI) of metallic nano-particles ascertained with the help of Malvern Nano sizer.

Zeta potential

The analysis of Zeta potential was accomplished with a motive of computing the stability of metallic nano-particles and elucidates the aggregation phenomenon of nano-particles (Horiba, Malvern Nano sizer).

X-ray Diffraction (XRD)

XRD studies manifests significant peaks ranging from 23.68° to 77.21°, which clearly verifies the crystalline nature of synthesized silver nano-particles. XRD and TEM results were confirmed with the nano-sized range of silver nano-particles. The gold nano-particles were found to be crystalline; this relation was established using XRD where three diffraction peaks were observed in the two-theta range of 30–80°, the particle size of the gold nano-particles formed had a particle size which was in good agreement with TEM results.

Antibacterial activity of synthesized metallic nano-particles¹³

To inspect the anti-bacterial properties of synthesized metallic nano-particles which are plant-mediated as opposed to the chosen microbes, agar well diffusion assay was used. The microbes that were tested were consistently dabbed on nutrient agar medium with the help of the loop of inoculum that was sterilized. Wells of diameter 6 mm were constructed by utilizing well borer of the capacity-100 µL of metallic nano-particles suspension with diverse strengths (30, 60, 90 and 120 µg mL⁻¹) gushed in the appropriate well. The mixture of Arvi was taken as a check specimen to ascertain the bactericidal attributes. At the temperature of 37°C, the plates were incubated for 24 h. The antibacterial attributes of metallic nano-particles were scrutinized with reference to the zone of inhibition.

Antioxidant activity of synthesized metallic nano-particles¹⁴

The antioxidant attributes of nano-particles were designated by utilizing assay of DPPH (2, 2-diphenyl-2-picrylhydrazyl hydrate). DPPH was used as stock solution; formed in methanol. 0.498 mL of nano-particles suspension of 25, 45, 65, 85 and 100 µg mL⁻¹ was mixed with 3 mL of ethyl alcohol and 0.3 mL of radical solution of DPPH. The reaction was briskly agitated and was permitted to stay undisturbed at 25 °C for 35 minutes. Incubating the specimen for 35 minutes, transformation from dark purple to yellowish white indicate that the mixture undergoes reduction. Now, with the help of UV-Visible spectrophotometer (SHIMADZU UV-1800), the absorbance was computed at 517 nm. The antioxidant attributes were evaluated by calculating the % inhibition by the formula given below:

$$\text{Percentage inhibition} = \frac{A_{\text{blank}} - A_{\text{sample}}}{A_{\text{blank}}} \times 100$$

RESULTS AND DISCUSSION

Observation and UV – Visible spectroscopy

Synthesis of metallic nano-particles was followed by means of transformation in colour and UV-Visible spectroscopy. The reaction mixture underwent a colour change from light white to brownish red (Fig. 1a) and also light white to violet (Fig. 1b). This suggests that silver and gold nano-particles have been synthesized, due to the metal ions that reduced into the metallic nano-particles

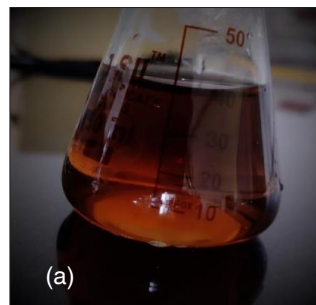


Fig. 1a: Reddish brown color depicting synthesis of silver nanoparticles

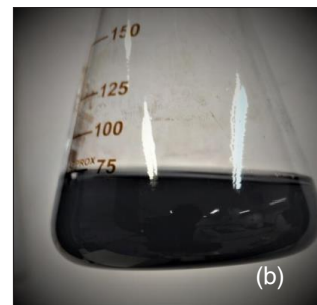


Fig. 1b: Purple color depicting synthesis of gold nanoparticles

by means of the chemically-active chemical components in the roots extract of Arvi¹⁵. The agitation of SPR is ascribed by reaction colour. Attributed to the expected property of SPR, the distinctive optical attributes exhibited by the noble metals¹⁶. A definite and expected SPR band for silver nano-particles is reported in scale of 350 – 450 nm (Fig. 2a and Fig. 2b). On the other hand, gold nano-particles have attained SPR bands in the scale of 450– 550 nm. The AgNO₃ and CA solutions are utilized as controls; brownish red color and violet color failed to appear correspondingly. Metal salts didn't portray the expected SPR band which indicated that metal salts failed to reduce when the reaction proceeds in the used conditions¹⁷.

Effects of concentration of the metal salts

The colour transformation from light yellow to brownish red and violet colour is noticed when strength of AgNO₃ and CA (2.48 and 1.48 mM) correspondingly was varied. SPR peaks of metallic nano-particles becomes significantly distinct on increasing the amount of metal salts. The peak intensity attains a maximum at concentration of 2 mM (Fig. 2a and Fig. 2b). The variation in the concentration of metal salt and biological components has significant impact on the nano-particles synthesis¹⁸.

Effects of the root extract of *C. esculenta*

The analysis of the SPR peaks revealed to be in direct proportionality relationship as the mass per unit density of

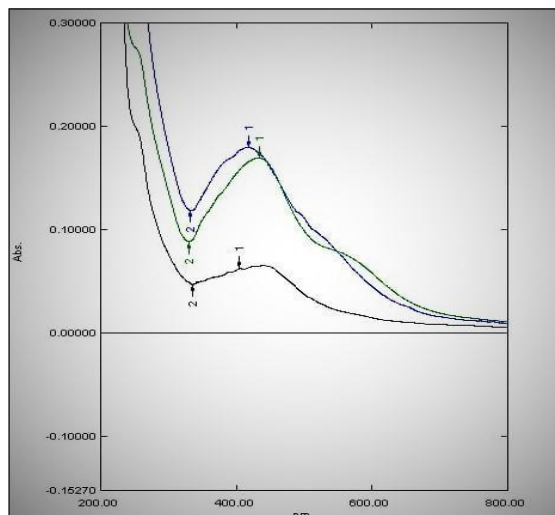


Fig. 2a: UV-Visible spectra of synthesized silver nanoparticles at varied concentrations of chloroauric acid

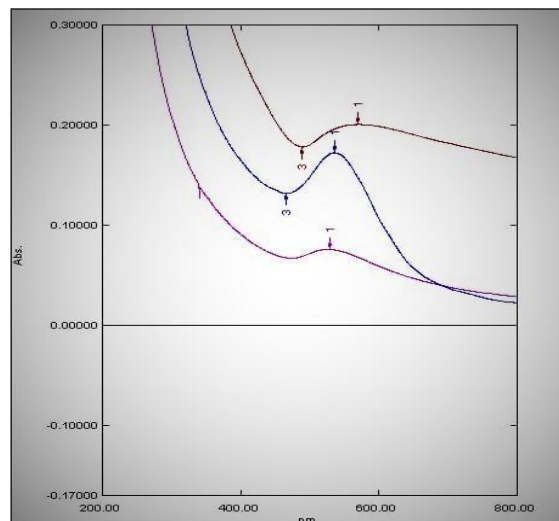


Fig. 2b: UV-Visible spectra of synthesized gold nanoparticles at varied concentrations of AgNO_3

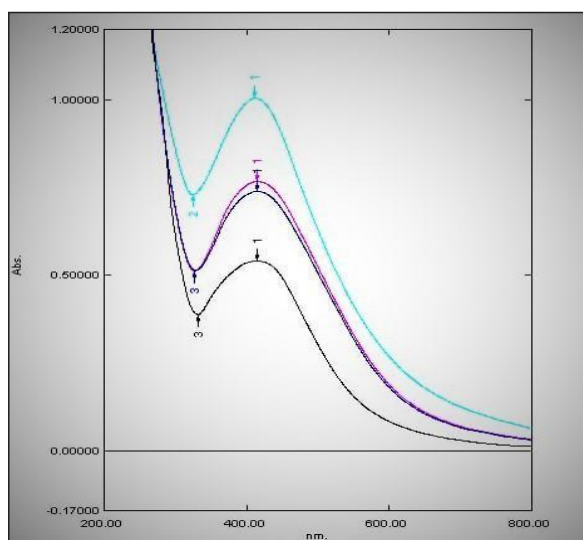


Fig. 2c: UV-Visible spectra of synthesized silver nanoparticles at differing volumes of *C. esculenta* root extract

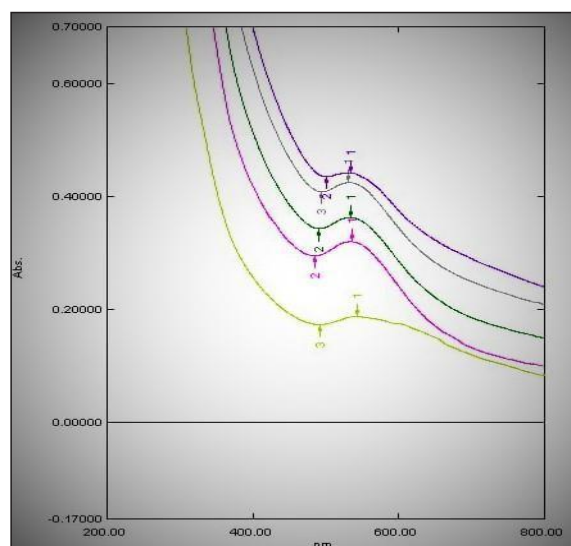


Fig. 2d: UV-Visible spectra of synthesized gold nanoparticles at differing volumes of *C. esculenta* root extract

root extract (in mL) surged (Fig. 2c and Fig. 2d). With the increase in the concentration of the biological components in the synthesis of metallic nano-particles increases, the higher number of components of the chemical origin present in the biological material is associated in the synthesis of metal reductive nano-particles¹⁹.

Effect of variation in pH

The quest of determining the pH of aqueous dispersion of silver nano-particles was conducted by using the instrument EQ-601 pH meter of Toschon Industries Pvt. Ltd. The colour of the reaction as well as the SPR peaks had intensities that were proportional to each other and intense. This implies that pH has a strong influence on

synthesis of metallic nano-particles. Thereafter, no colour changes were observed. In addition, a precipitate which was white in colour was reported at pH value ranging between 1 – 3. For pH values lying in the range 5 – 9 for silver and gold nano-particles correspondingly; diverse tints of reddish-brown and purple color (Fig. 3a and Fig. 3b) were observed. The reaction was then allowed to proceed at an acidic pH ranging between 1 – 3; no colour transformation was seen. Moreover, the SPR peaks were reported to have the usual characteristic curves. The diverse biomolecules contained in the biological material are associated with the synthesis of the biological nano-particles, such as biomolecules are probable to be disabled under the impact of extremely acidic reaction conditions²⁰.

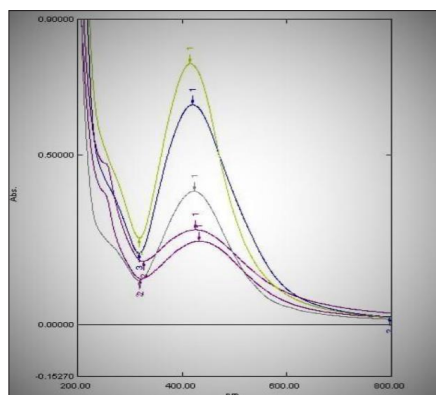


Fig. 3a: UV-Visible spectra of synthesized gold nano-particles at various pH values

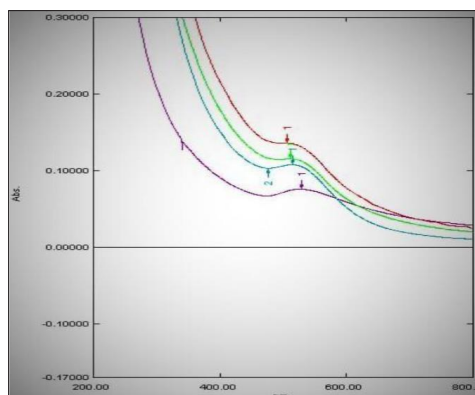


Fig. 3b: UV-Visible spectra of synthesized silver nano-particles at various pH values

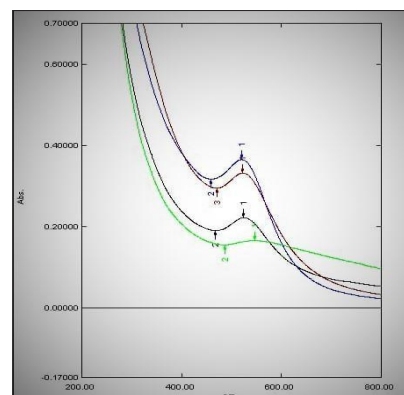


Fig. 3c: UV-Visible spectra of synthesized gold nano-particles at varied temperature conditions

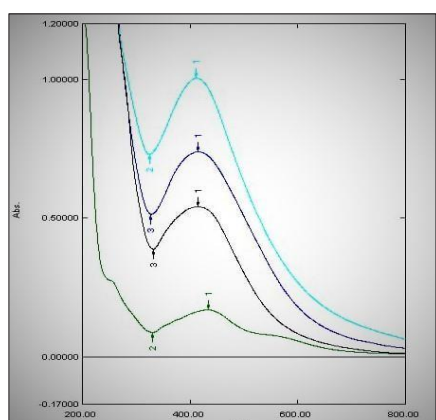


Fig. 3d: UV-Visible spectra of synthesized silver nano-particles at varied temperature conditions

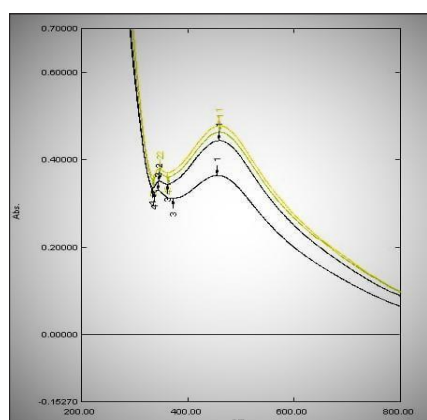


Fig. 3e: UV-Visible spectra of synthesized silver nano-particles at varied incubation times

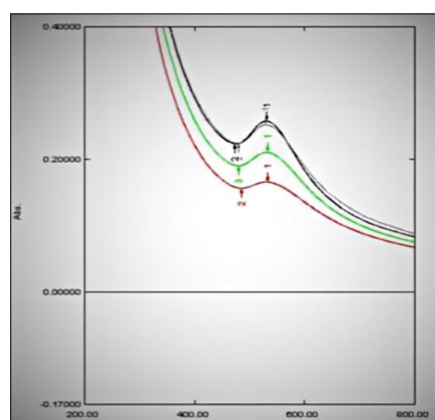


Fig. 3f: UV-Visible spectra of synthesized gold nano-particles at varied incubation times

The diversifications observed in the intensities of colour observed upon the change in the values of pH can be hypothesized and the variation observed in the values of dissociation constants (pK_a) of the concerned functional groups that are associated²⁰.

Results of variation in reaction temperature

The reaction temperature put forth a significant impact on synthesis of metallic nano-particles. After incubation at temperatures 30 °C and 45 °C exhibited whitish yellow and light violet color for silver and gold nano-particles correspondingly and then SPR peaks had intensities that were statistically insignificant. At significantly higher temperatures (65, 85 and 95°C) of the reaction, dark reddish-brown and purple color appeared for silver and gold nano-particles respectively. Peaks observed in SPR have intensities that are statistically significant. At room temperature, the transformation of colour required 60 minutes to appear. On the other hand,

at higher temperatures, reduction was observed to occur rapidly and transformation of colour appeared within 25 minutes. The sharpness of the SPR peak reaches its maximum at 100 °C (Fig. 3c and 3d). UV spectra reflect narrow and sharp peaks at low wavelengths with a rise in reaction temperature. This demonstrates the synthesis of metallic nano-particles that are smaller in size. On the other hand, at lower temperatures, the peaks of SPR are sharp at higher wavelengths highlighting the formation of metallic nano-particles that are large in size, as depicted by UV spectra. UV Visible Spectra of the synthesized silver and gold nano-particles respectively at varied incubation time is also shown (Fig. 3e and 3f). We can ascertain that the reactants are used up swiftly with the rise in reaction temperature; which ultimately lead to the synthesis of metallic nano-particles smaller in size²¹. In a nutshell, we can ascertain that the absolute size of the metallic nano-particles was significantly lowered with a rise in temperature of the reaction.

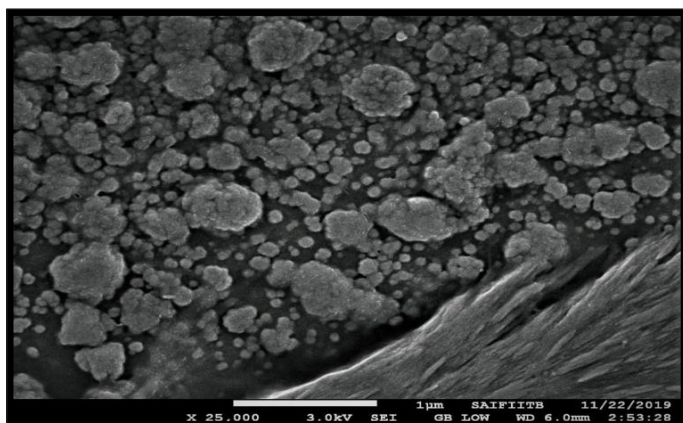


Fig. 4a: FESEM illustrations of synthesized silver nano-particles

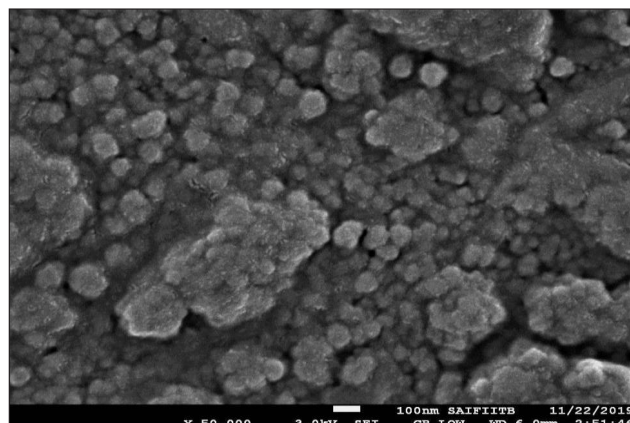


Fig. 4b: FESEM illustrations of synthesized gold nano-particles

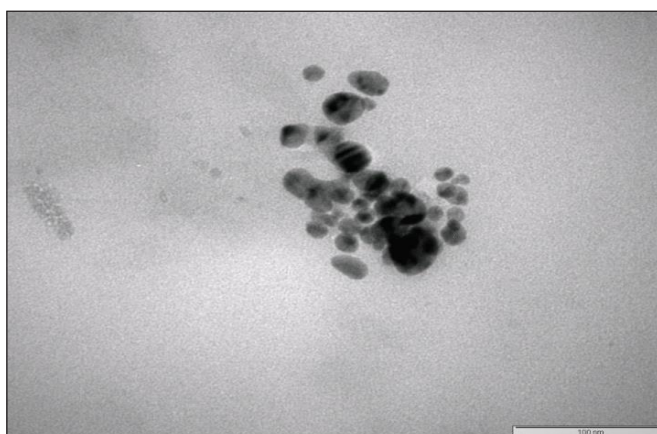


Fig. 4c: TEM descriptions of synthesized silver nano-particles

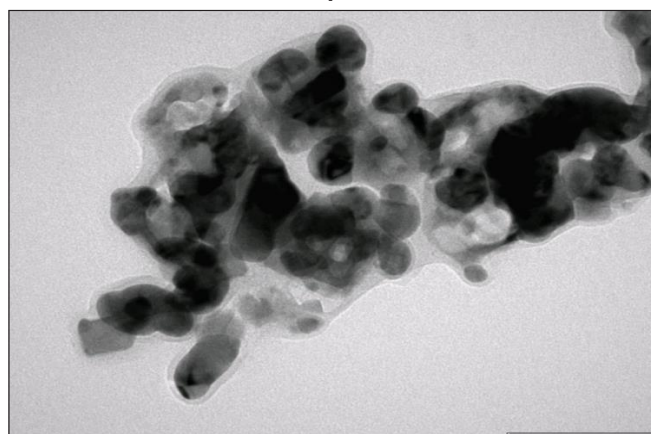


Fig. 4d: TEM descriptions of synthesized gold nano-particles

Result of variation in incubation time

By progression of incubation time of reaction, the color intensity keeps, increasing, representing the fact that the process of reduction was slow at the start of the reaction and moderately fastens as the incubation time proceeds. The graph peaks were found to be deeper and the results were as expected after longer incubation time i.e., 96 h (Fig. 1a and Fig. 1b). The reduction of most of the metal ions was attained after the incubation time reached 96 h. With the increase in incubation time, the progress in the absorbance accompanying changing color intensity is essentially dependent on an increase in formation of metallic nano-particles²². The swift synthesis of the metallic nano-particles can be owed to the statistically important reduction potential of the root extracts of *C. esculenta* and their ability to stabilize within a spectrum of narrow size²².

Characterization of silver nano-particles

Form of the metallic nano-particles was meticulously examined using FESEM. The illustration procured utilizing

FESEM portrayed spherical and monodispersed metallic nano-particles (Fig. 4a and Fig. 4b). The TEM illustrations obtained show that the metallic nano-particles being monodispersed are spherical (Fig. 4c and Fig. 4d). The metallic nano-particles are obtained as pure crystals. The Z-average, PDI, zeta potential of nano-particles examined using Dynamic Light Scattering (DLS) (Table I, Fig. 5 a, b, c and d). XRD pattern of silver and gold nano-particles biosynthesized by the utilization of *C. esculenta* root extract respectively are shown in Fig. 6a and b.

Antimicrobial activity of metallic nano-particles

Agar well diffusion method has a unique position in determining the antibacterial property of the metallic nano-particles²³. Metallic nano-particles demonstrated antimicrobial activity as opposed to the microbes²⁴. The metallic nano-particles portrayed variable intensities of bactericidal activity as opposed to microbes, which was obtained by the diameter of inhibition zone. In addition, the seed extract of *C. esculenta* failed to exhibit bactericidal activity²⁵.

Table I: Z-average, PDI and zeta potential of biosynthesized silver and gold nano-particles from the root extract of *C. esculenta*

Metallic nano-particles	Z-average (in nm)	PDI	Zeta potential (in mV)
Silver nano-particles	101.2	0.724	-28.981
Gold nano-particles	84.8	0.812	-25.894

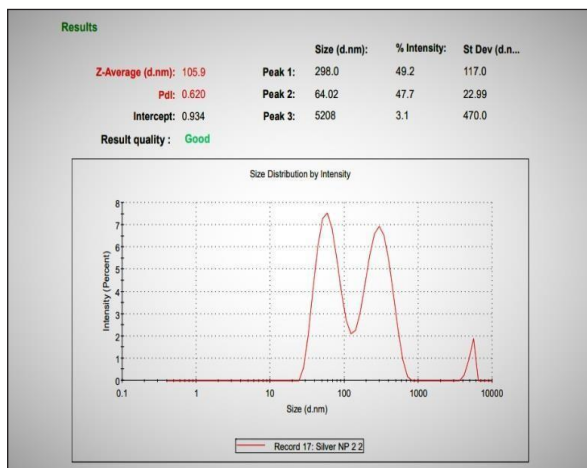


Fig. 5a: Particle size of synthesized silver nano-particles

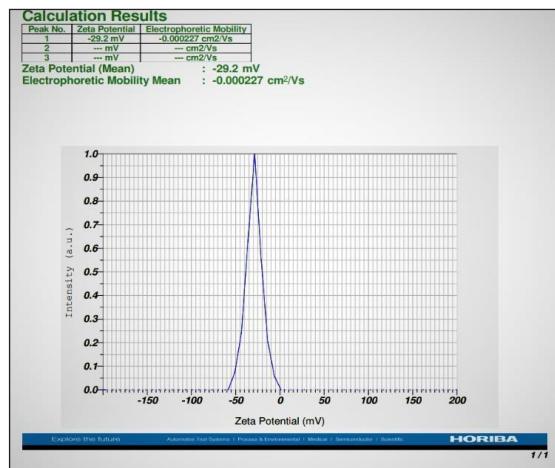


Fig. 5b: Zeta potential of silver nano-particles

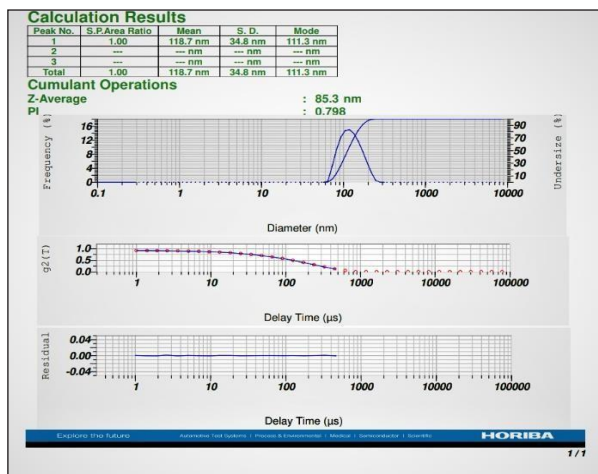


Fig. 5c: Particle size of synthesized gold nano-particles

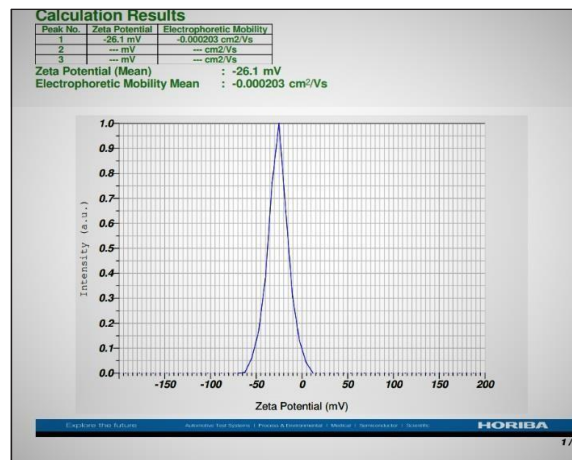


Fig. 5d: Zeta potential of synthesized gold nano-particles

Diverse mechanisms are hypothesized for the properties of synthesized metallic nano-particles to kill bacteria as opposed to microbes²⁶.

1. The metallic nano-particles have the tendency to modify the cell surface with a negative charge by adjusting the physico-chemical attributes of the plasma membrane and cell wall; perturbing primary tasks of the cell like osmoregulation, adenosine triphosphate (ATP) synthesis and cell permeability²⁷.
2. The metallic nano-particles react with the

Deoxyribonucleic acid (DNA), sulphur and phosphorus possessing cell elements and proteins by penetrating the cell; hence damaging the cells of bacteria²⁸.

3. The metallic nano-particles initiate an escalated bactericidal activity by liberating metal ions which are dependent on size and dose²⁹.

The antibacterial properties with varying strengths of silver and gold nano-particles (60, 120 and 180 $\mu\text{g mL}^{-1}$) were determined with reference to the diameter of inhibition zone against the pathogenic

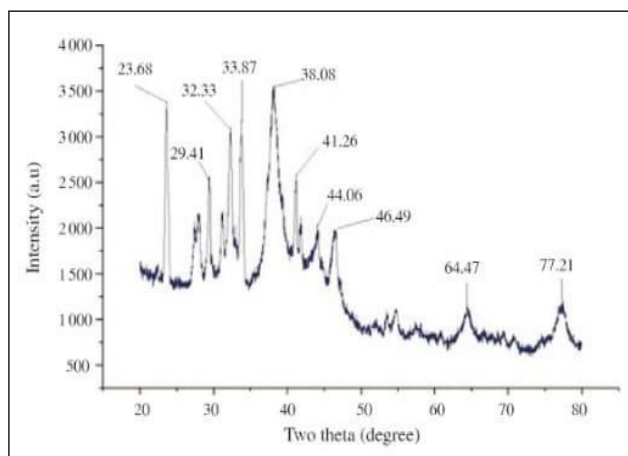


Fig. 6a: XRD pattern of silver nano-particles synthesized utilizing *C. esculenta* roots extract

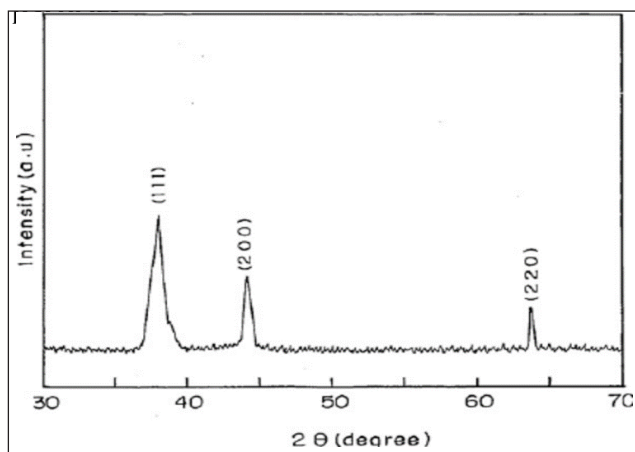


Fig. 6b: XRD pattern of gold nano-particles synthesized utilizing *C. esculenta* roots extract

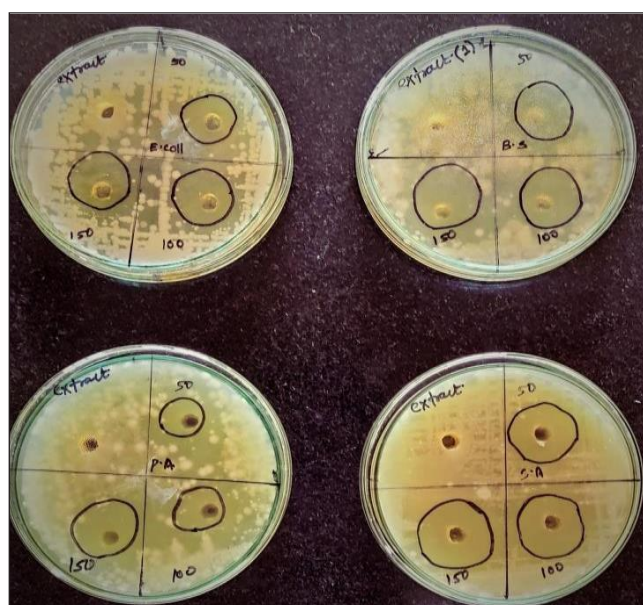


Fig. 6c: Antimicrobial activity of synthesized silver nano-particles as opposed to *E. coli*, *S. aureus*, *P. aeruginosa* and *B. subtilis*



Fig. 6d: Antibacterial activity of synthesized gold nano-particles as opposed to *E. coli*, *S. aureus*, *P. aeruginosa* and *B. subtilis*

Table II: Antimicrobial activity of synthesized silver nano-particles against pathogenic microbes and its critical assessment with regard to the inhibition zone measures (in mm)

For silver nano-particles	Diameter of zone of inhibition (in mm)			
	<i>E. coli</i>	<i>S. aureus</i>	<i>B. subtilis</i>	<i>P. aeruginosa</i>
Microbe used				
Concentration ($\mu\text{g mL}^{-1}$)				
60	21	24	24	17
120	27	26	25	19
180	24	28	26	23

Table III: Antimicrobial activity of biosynthesized gold nano-particles against representative pathogenic microorganisms and its evaluation in terms of the inhibition zone measures (in mm)

For gold nano-particles	Diameter of zone of Inhibition (in mm)			
Microbes used	<i>E. coli</i>	<i>S. aureus</i>	<i>B. subtilis</i>	<i>P. aeruginosa</i>
Concentration ($\mu\text{g mL}^{-1}$)				
60	22	24	22	20
120	25	26	24	22
180	27	29	25	24

Table IV: Antioxidant activity (in % inhibition) exhibited by synthesized silver nano-particles as a test in contrast to standard ascorbic acid

Sr. No.	Concentration ($\mu\text{g mL}^{-1}$)	Antioxidant activity of biosynthesized silver nano-particles (in %)	Antioxidant activity of ascorbic acid (in %)
1	15	67.98	70.83
2	30	78.89	82.78
3	45	85.78	87.64
4	60	89.74	90.65
5	95	91.82	93.57

Table V: Antioxidant activity (in % inhibition) exhibited by synthesized gold nano-particles as a test in contrast to standard ascorbic acid

Sr. No.	Concentration ($\mu\text{g mL}^{-1}$)	Antioxidant activity of synthesized gold nano-particles (in %)	Antioxidant activity of ascorbic acid (in %)
1	15	56.85	70.58
2	30	63.69	82.74
3	45	68.78	87.59
4	60	72.96	90.67
5	95	81.21	93.87

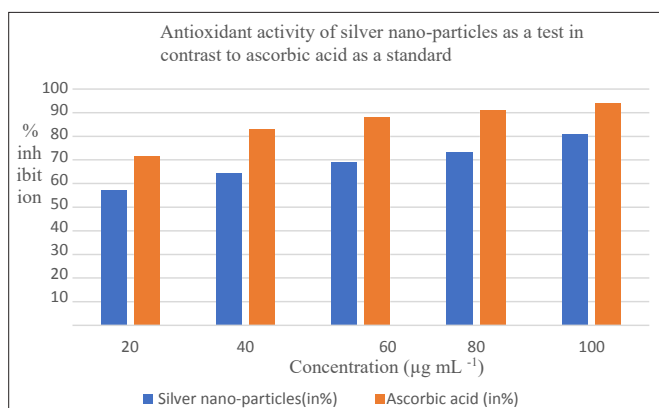


Fig. 7a: Antioxidant activity of silver nano-particles as a test in contrast to standard ascorbic acid

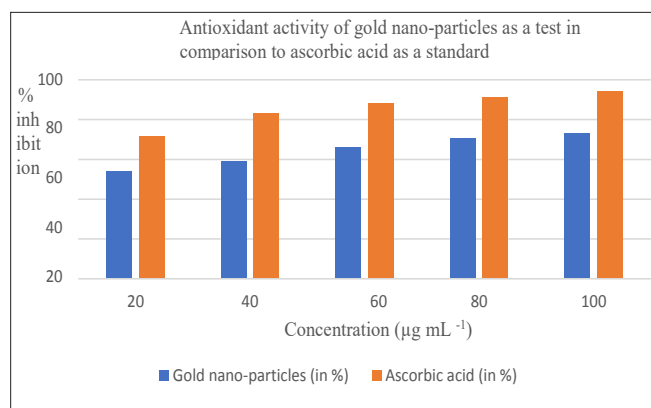


Fig. 7b: Antioxidant activity of gold nano-particles synthesized using green synthesis method as a test in contrast to standard ascorbic acid

microorganisms³⁰ (Fig. 6 c and d). The average diameter of the zone of inhibition (in mm) shown by the silver and gold nano-particles as opposed to the chosen microbes are given in Table II and Table III.

Antioxidant activity of synthesized nano-particles

The synthesized metallic nano-particles contain free-radical scavenging activity as opposed to DPPH; portrayed through the color transformation from the colour purple to yellow³¹. The antioxidant activities exhibited by the synthesized metal nano-particles were compared with the antioxidant activities of standard ascorbic acid. The observation reporting the antioxidant activities of synthesized metallic nano-particle surged as the molarity of metallic nano-particles increased from 15 µg mL⁻¹ to 95 µg mL⁻¹³². The differential analysis is also shown (Table IV, V and Fig. 7a, b).

CONCLUSION

The roots of *C. esculenta* are ideally suited for the swift and feasible production of metallic nano-particles. The metallic nano-particles produced using green synthesis method utilizing the seed extract of *C. esculenta* underwent critical characterization. The Zeta potential and Z-average size of silver nano-particles were monitored having values such as 105.07 nm and -28.9 mV, respectively; on the other hand, for gold nano-particles the values were documented to be 84.9 nm and -25.98 mV, respectively. XRD studies demonstrated remarkable peaks ranging from 23.68° to 77.21° of synthesized silver nano-particles whereas for gold nano-particles the peaks were reported. in the range of 30–80°; this clearly substantiates that the synthesized nano-particles are crystalline. The metallic nano-particles appeared spherical, similar to each other, monodispersed and crystalline. The scrutinization of anti-microbial properties revealed that the metallic nano-particles exhibited statistically significant anti-microbial properties as opposed to the chosen microbes. DPPH investigation portrayed that synthesized metallic silver and gold nano-particles reflected statistically significant antioxidant properties as opposed to DPPH and its properties were differentiated by using ascorbic acid as a standard. The bottom line is that green synthesis has exemplary benefits over other contemporary processes due to its being ecologically safe and inexpensiveness; this synthesis method can also be exploited for the bulk manufacture of nano-particles.

REFERENCES

1. Saeid F., Moradnia F. and Ramazani A.: Green synthesis and characterization of ZnMn₂O₄ nano-particles for

- photocatalytic degradation of Congo red dye and kinetic study. **Micro Nano Lett.**, 2019, 14(9), 986-991.
2. Saeid F., Forootan R., Moradnia F., Afshari Z. and Ramazani A.: Green synthesis, characterization, and photocatalytic activity of cobalt chromite spinel nano-particles. **Mater. Res. Express**, 2020, 7(1).
3. Saeid F., Moradnia F., Moradnia S., Forootan R., Zare F. Y. and Heidari M.: Eco-friendly synthesis and characterization of α-Fe₂O₃ nano-particles and study of their photocatalytic activity for degradation of Congo red dye. **Chem. Methodol.**, 2019, 3(6), 684-795.
4. Saeid F., Moradnia F., Ghalaichi A. H., Pajouh S. D. and Heidari M.: Facile green synthesis and characterization of zinc oxide nano-particles using tragacanth gel: investigation of their photocatalytic performance for dye degradation under visible light irradiation. **Nanochem. Res.**, 2020, 5, 69-76.
5. Saeid F., Moradnia F., Mostafaei M., Afshari Z., Faramarzi V. and Ganjkanlu S.: Biosynthesis of MgFe₂O₄ magnetic nano-particles and its application in photo-degradation of malachite green dye and kinetic study. **Nanochem. Res.**, 2019, 4(1), 86-93.
6. Saeid F., Ramazani A. and Sang W. J.: Sol-gel Synthesis and Characterization of Zinc Oxide Nano-particles Using Black Tea Extract. **J. Appl. Chem.**, 2018, 59(7), 1730-1736.
7. Moradnia F., Saeid F. T., Ramazani A., Osali S. and Abdolmaleki I.: Green sol-gel synthesis of CoMnCrO₄ spinel nano-particles and their photocatalytic application. **Nanochem Res.**, 2019, 4(2), 140-147.
8. Ahmad A., Mukherjee P., Senapati S., Mandal D., Khan M. I., Kumar R., Sastry Rajiv and Murali: Extracellular biosynthesis of silver nano-particles using the fungus *Fusarium oxysporum*. **Colloids Surf.**, 2003, 28, 313-318.
9. Rani A. and Valiyaveetil S.: Cytotoxicity and genotoxicity of silver nano-particles in human cells. **ACS Nano**, 2009, 3, 279-290.
10. Azmath P., Baker S., Rakshith D. and Satish S.: Mycosynthesis of silver nano-particles bearing anti-bacterial activity. **Saudi Pharm J.**, 2016, 24(2), 140-146.
11. Atindehou K., Kone M., Terreaux C., Traore D., Hostettmann K. and Dosso M.: Evaluation of the antimicrobial potential of medicinal plants from the Ivory Coast. **Phytother. Res.**, 2002, 16(5), 497-502.
12. Subbaiya R. and Ponmurugan P.: Green synthesis of silver nano-particles from leaf extract *Azadirachta indica* and to study its antibacterial and antioxidant property. **Int. J. Curr. Microbiol. Appl. Sci.**, 2013, 2(6), 228-235.
13. Syed B, Prithvi S., Bisht N., Nikhil K., Davronov F.R., Aishwarya T., Ashwini P., Satish S., S., Nanjundaswamy M. N. and Nagendra P.: Phytobiological Mediated Production of Silver Nano-particles from *Colocasia esculenta* and their Bactericidal Potential. **J. Biol. Act. Prod. Nat.**, 2018, 3, 154-161.
14. Bhainsa K., and D'Souza S.: Extracellular biosynthesis of silver nano-particles using the fungus *Aspergillus fumigatus*. **Colloids Surf.**, 2006, 47, 160-164.

15. Bindhu, M. and Umadevi M.: Synthesis of monodispersed silver nano-particles using Hibiscus cannabinus leaf extract and its antimicrobial activity. **Spectrochim. Acta A. Mol. Biomol.**, 2013,101, 184-190.
16. Chia C., Yang H. Wen M. and Chern C.: Estimation of total flavonoid content in propolis by two complementary colorimetric methods. **J. Food Drug Anal.**, 2002,10(3), 178-182.
17. Kuppastl., Virupaksha J. and Ravi M.: A review on *Colocasia esculenta*. **Int. J. Univers. Pharm. Bio Sci.**, 2014, 3(6), 309-321.
18. Edeoga H., Okuw D. and Mbaebie B.: Phytochemical constituents of some Nigerian medicinal plants. **Afr. J. Biotechnol.**, 2005, 4(7), 685-688.
19. Rafiee H., Yari S, Pourghadir M. and Abdousi V.: A review: Silver Nano-particles Synthesis through plants income parison with chemical and biological methods. **Fire, Int. J. Eng. Technol.**, 2015, (1), 278- 285.
20. Ibrahim H.: Green synthesis and characterization using Arvi peel extract and their antimicrobial activity against representative microorganisms. **Radiat. Res. Appl. Sci.**, 2015, (5), 1-11.
21. Patel I., Kara H, et al.; Arvi extract synthesized silver nano-particles have higher stability as compared to orange extract synthesized silver nano-particles. **J. Med. Chem.**, 2015, (6), 218-227.
22. Tang J., Xiong L., Wang S., Wang J., Liu L., Li. J, Wan Z. and Xi T.: Influence of silver nano-particles on neurons and blood-brain barrier via subcutaneous injection in rats. **Appl. Sci.**, 2008, 255(2), 502-524.
23. Song J. and Kim B.: Rapid biological synthesis of silver nano-particles using plant leaf extracts. **Bioprocess Biosyst. Eng.**, 2009, 32, 79-84.
24. Liu J., Sonshine D., Shervani S. and Hurt R.: Controlled release of biologically active silver from nanosilver surfaces. **ACS Nano**, 2010, 4, 6903-6913.
25. Marambio J. and Hoek E.: A review of the antibacterial effects of silver nanomaterials and potential implications for human health and the environment. **J. Nanopart. Res.**, 2010, 12, 1531-1551.
26. Gangwar M., Gautam M., Sharma A. K., Tripathi Y. B., Goel R. K. and Nath G.: Antioxidant capacity and radical scavenging effect of polyphenol rich *Mallotus philippensis* fruit extract on human erythrocytes: *In vitro* study. **Sci. World J.**, 2014, (10), 1-12.
27. Dike M., Anerao R. and Thergaonkar M.: Synthesis of gold nanostructures using fruit extract of *Colocasia esculenta*. **Int. J. Cosmet. Sci.**, 2013, 3, 34-39.
28. Krishnaprabha M. and Manjunatha P.: Synthesis of Gold Nano-particles Using *Colocasia esculenta* Fruit Rind Extract. **Int. J. Nanosci.**, 2016, 15, 1-6.
29. Vanaja M., Paulkumar K., Gnanajobitha G., Rajeshkumar S., Malarkodi C. and Annadurai G.: Herbal plant synthesis of Antibacterial silver nano-particles by *Solanum trilobatum* and its characterization. **Int. Met. Rev.**, 2014, (6), 1-9.
30. Nanda A. and Saravanan M.: Biosynthesis of silver nano-particles from staphylococcus aureus and its antimicrobial activity against MRSA and MRSE. **Nanomed. J.**, 2009, (5), 452- 456.
31. Nel, A., Madler, L., Velegol, D., Xia T., Hoek E., Somasundaran, P., Klaessig F., Castranova V. and Thompson M.: Understanding biophysicochemical interactions at the nano-bio interface **Nat. Mater.**, 2009, (8), 543-557.
32. Salata O.: Applications of nano-particles in biology and medicine. **J. Nanobiotechnology**, 2004, (2), 1-6.



For Advertising in the Classified Columns and also for series advertisements please contact: Geeta Suvarna (+9820161419)

Publications Department

IDMA BULLETIN

Tel.: 022 - 2494 4624 / 2497 4308 E-mail: publications@idmaindia.com

Website: www.idma-assn.org, www.indiandrugsonline.org